Evolution of the micromechanical properties of impacted granular materials

Franck Bourrier, François Nicot, Félix Darve

▶ **To cite this version:**

Franck Bourrier, François Nicot, Félix Darve. Evolution of the micromechanical properties of impacted granular materials. Comptes Rendus Mécanique, 2010, 338 (10-11), pp.639-647. 10.1016/j.crme.2010.09.007 . hal-02594602

HAL Id: hal-02594602
https://hal.inrae.fr/hal-02594602v1

Submitted on 18 Sep 2024

HAL is a multi-disciplinary open access archive for the deposit and dissemination of scientific research documents, whether they are published or not. The documents may come from teaching and research institutions in France or abroad, or from public or private research centers.

L'archive ouverte pluridisciplinaire **HAL**, est destinée au dépôt et à la diffusion de documents scientifiques de niveau recherche, publiés ou non, émanant des établissements d'enseignement et de recherche français ou étrangers, des laboratoires publics ou privés.

Distributed under a Creative Commons Attribution - NonCommercial 4.0 International License

Evolution of the micromechanical properties of impacted granular materials

Evolution des propriétés micro-mécaniques de matériaux granulaires sous impact

Franck Bourrier [a,*], François Nicot [a], Felix Darve [b]

[a] *Cemagref, UR EMGR, 38402 St-Martin d'Hères cedex, France*
[b] *L3S-R, UMR5521, INPG-UJF-CNRS, DU Grenoble Universités, 38041 Grenoble cedex 9, France*

The impact of a projectile on a granular material induces important changes in the micromechanical properties of the impacted material. These changes are studied using a Discrete Element Method model of the impact. The numerical results show that the impact first entails an energy propagation from the impact point to the limit of the sample through the existing force chains. A significant kinetic energy and a total breakage of the existing contact force chains are the main consequences of the energy propagation. During the long recovery balance phase observed after the energy propagation phase, frictional processes cause the kinetic energy dissipation. The motions of the particles and the numerous contact openings first prevent the formation of stable force chains. However, for long durations after the beginning of the impact, contact openings stop. The balance recovery phase therefore finally results in the creation of new stable contact force networks.

L'impact d'un projectile sur un matériau granulaire entraîne d'importants changements des propriétés micro-mécaniques du matériau impacté. Ces changements sont étudiés à l'aide d'un modèle d'impact basé sur la Méthode des Eléments Discrets. Les simulations mettent en évidence que l'impact conduit tout d'abord à une propagation d'énergie du point d'impact vers les limites de l'échantillon impacté le long des chaînes de forces existantes. Cette propagation d'énergie conduit à la destruction des réseaux de forces existants et à l'augmentation significative de l'énergie cinétique en tout point de l'échantillon. Durant la longue phase de retour à l'équilibre suivant la propagation d'énergie, l'énergie cinétique est dissipée par frottement. Les mouvements des particules et les nombreuses ouvertures de contacts empêchent tout d'abord la formation de chaînes de forces stables. Dans un second temps, les ouvertures de contact cessent, ce qui permet la formation de nouveaux réseaux de forces stables et, par conséquent, le retour à l'équilibre de l'échantillon.

* Corresponding author.
E-mail addresses: franck.bourrier@cemagref.fr (F. Bourrier), francois.nicot@cemagref.fr (F. Nicot), felix.darve@inpg.fr (F. Darve).

Accepted Manuscript

1. Introduction

In many engineering problems, the issue of impacting bodies emerges. From an academic point of view, this problem is strongly related with the modelling of the interfacial mechanisms occurring between the two contacting bodies [1–4]. This article deals with this issue, in the specific case of the impact of a sphere on a granular assembly, which was also extensively studied in relation with various research fields [5–10]. The practical motivation of this work concerns rockfall hazard assessment. In the field of rockfall hazard assessment, many scientific problems related with falling rocks trajectory simulations, and in particular with the bouncing of the falling rocks on the slope surface, remain to be solved. Modelling the bouncing of falling rocks on a soil requires the identification of the causes of the bouncing and of the mechanisms involved in the dynamic interaction between the rock and the soil.

Models based on the Discrete Element Method (DEM) are particularly relevant to integrate the discrete nature of the impacted material and the dynamic loadings [5–7,11]. Numerical studies using the DEM [11] have shown that the rebound is closely related with energy transfers between the projectile and the soil. As a step further in the understanding of the interaction between a projectile and a granular material, this paper focuses on the energy transfers inside the granular material and on the evolution of the micromechanical properties of the granular assembly during the impact. A discrete model of the impact is developed in the case of the normal impact of a projectile of the same size as the mean size of the material particles. Based on the analysis of the evolution of the energy transfers and of the micromechanical properties of the material, the successive physical processes associated with the energy propagation and with the balance recovery inside the material are detailed.

2. Modelling the impact

2.1. Discrete Element Method model

The model of the impact was developed using the Particle Flow Code 2D software [12], which is based on a Discrete Element Method (DEM – [13]). The DEM method assumes that the impacted material is a collection of rigid locally deformable bodies. The interactions between particles are described by force-displacement contact models. In the solving scheme, particles locations are listed. Interaction forces between particles are then determined from particles locations. Finally, an explicit algorithm allows solving Newton's second law for the calculation of the particles' translational and rotational velocities. The calculated velocities are used to determine new particles locations for the next time step.

In the model presented, the interactions between particles are governed by a contact model [14] based on an approximation of the Hertz–Mindlin theory [15]. The contact model formulation relates both the normal and tangential incremental contact forces $\mathrm{d}F_n$ and $\mathrm{d}F_t$ to the normal and the tangential incremental interpenetrations $\mathrm{d}u_n$ and $\mathrm{d}u_t$ using the relations:

$$\mathrm{d}F_n = \frac{3}{2} K_n \sqrt{u_n}\, \mathrm{d}u_n \tag{1}$$

$$\mathrm{d}F_t = K_t\, \mathrm{d}u_t\, \xi(F_n \tan\varphi - F_t) \tag{2}$$

with

$$K_n = \frac{2\sqrt{2\bar{R_p}}\bar{G}}{3(1-\bar{\nu})} \tag{3}$$

$$K_t = 2\frac{(3\bar{G}^2(1-\bar{\nu})\bar{R_p})^{1/3}}{2-\bar{\nu}} F_n^{1/3} \tag{4}$$

where φ is the local friction angle, K_n et K_t are the normal and tangential stiffnesses depending on the harmonic mean of the radius $\bar{R_p}$, on the arithmetic mean of the shear modulus $\bar{G}$ and of the Poisson ratio $\bar{\nu}$ of the particles. ξ is the Heaviside function: $\xi(x) = 1$ if $x > 0$ and $\xi(x) = 0$ if $x \leqslant 0$.

The interaction force model only includes energy dissipation through frictional processes. No additional viscous or inertial damping coefficients introducing other energy dissipation types were used in the simulations. In the simulations, the assumption is therefore made that the energy transfers and dissipation associated with particle rearrangement are predominant compared with other dissipation processes. The relevant numerical modelling of energy dissipation in real systems is still an open question and no clear conclusions exist on the contact model to be used in Discrete Element Methods. In particular, classical discrete numerical models of granular materials do not account in a relevant manner for contact attrition, local particle breakage, heat energy dissipations and energy dissipation due to high frequency wave propagation.

The impacted material is modelled as a polydisperse granular assembly. The properties of the assembly are defined to match classical values in the context of the impact of a rock on a coarse soil. The mean radius of the particles is $R_m = 0.3$ m and the ratio between the mass of the smaller particles and larger particles is set at 10. The properties of the particles are set at classical values for rocks [16]: $\rho_m = 2650$ kg/m^3, $G = 40$ GPa, $\nu = 0.25$, $\varphi = 30°$.

The soil sample (Fig. 1) is generated from distinct particles subjected to gravitational forces only. Gravitational forces are applied to all particles and a calculation procedure is run until the total kinetic energy of the system lowers a set value.

Accepted manuscript

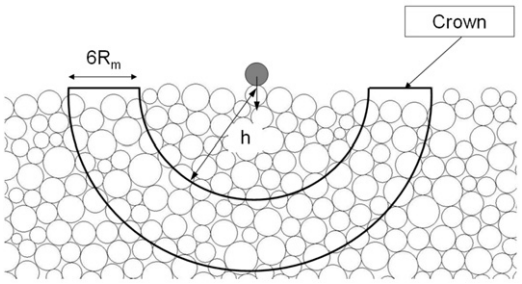

Fig. 1. Definition of concentric crowns.

The porosity of the sample is controlled by the value of the local friction angle during the generation process. During the generation phase, the local friction angle was set at 0° to obtain a dense assembly. In addition, during this phase, local viscous damping on the normal component of the contact forces was introduced to facilitate the assembly stabilization. After sample generation, the local friction angle is set at $\varphi = 30°$, sample depth is set at $50R_m$ and sample length is set at $100R_m$. The size of the sample was determined in order to avoid interactions between the initial energy propagation and energy reflection on the boundaries of the sample. However, although the physical processes described in the followings are similar for any sample size, the quantitative values of the results obtained may depend on the size of the sample. Additional details on the properties of the assembly can be found in [11].

The projectile radius R_p is set at the same value as the mean radius of the particles R_m. This size ratio corresponds to the impact of rocks on coarse granular soils classically encountered on talus slopes. This article focuses on normal impacts of projectiles without rotational velocity before impact. The incident velocity of the projectile is set at $V^{in} = 20$ m/s which corresponds to classical values for falling rocks [17].

2.2. Energy calculation

For each timestep, all energies associated with both the projectile and the granular assembly were calculated with special focus on the energies transferred within the material. For a given domain D of the material composed with $N_b(t)$ particles and $N_c(t)$ contacts, these energetic quantities are the total kinetic energy $E_k(D)$, the total strain energy $E_s(D)$ and the total variation of the gravitational energy. As shown in [11], the total variation of the gravitational energy is negligible compared with the other energies. The total kinetic energy $E_k(D)$ inside the domain (D) is calculated as follows:

$$E_k(D) = \sum_{j=1}^{N_b(t)} \left(\frac{1}{2} M_j V_j^2(t) + \frac{1}{2} I_j \omega_j^2(t) \right) \tag{5}$$

where $V_j(t)$ is the velocity of the jth particle at time t, I_j is the inertia momentum of the jth particle and $\omega_j(t)$ is the rotational velocity of the jth particle.

For the calculation of the total strain energy $E_s(D)$, the assumption is made that the tangential interpenetration increment $\mathrm{d}u_{t,j}(t)$ at the jth contact can be separated into an elastic increment $\mathrm{d}u^e_{t,j}(t)$ and a plastic increment $\mathrm{d}u^p_{t,j}(t)$ defined as follows:

$$\mathrm{d}u^p_{t,j}(t) = \mathrm{d}u_{t,j}(t) - \mathrm{d}u^e_{t,j}(t) \tag{6}$$

with

$$\mathrm{d}u^e_{t,j}(t) = \frac{\mathrm{d}F_{t,j}(t)}{K_t} \tag{7}$$

The elastic strain energy $E_s(D)$ associated with the $N_c(t)$ contacts inside the domain D is calculated incrementally:

$$\mathrm{d}E_s(D) = \sum_{j=1}^{N_c(t)} \left(F_{n,j}(t)\, \mathrm{d}u_{n,j}(t) + F_{t,j}(t)\, \mathrm{d}u^e_{t,j}(t) \right) \tag{8}$$

where $F_{n,j}(t)$ (resp. $F_{t,j}(t)$) is the normal (resp. tangential) component of the contact force associated with the jth contact of (D) at time t; $\mathrm{d}u_{n,j}(t)$ is the normal interpenetration increment associated with the jth contact.

In the context of this study, the energy is transferred to the granular assembly at a fixed location corresponding to the impact point. Concentric crowns (Fig. 1) centred on the impact point are therefore chosen as domains D to analyze the energy transfers inside the material. The concentric crowns are located at distances h from the impact point. The thickness of these crowns is set at $6R_m$.

Accepted Manuscript

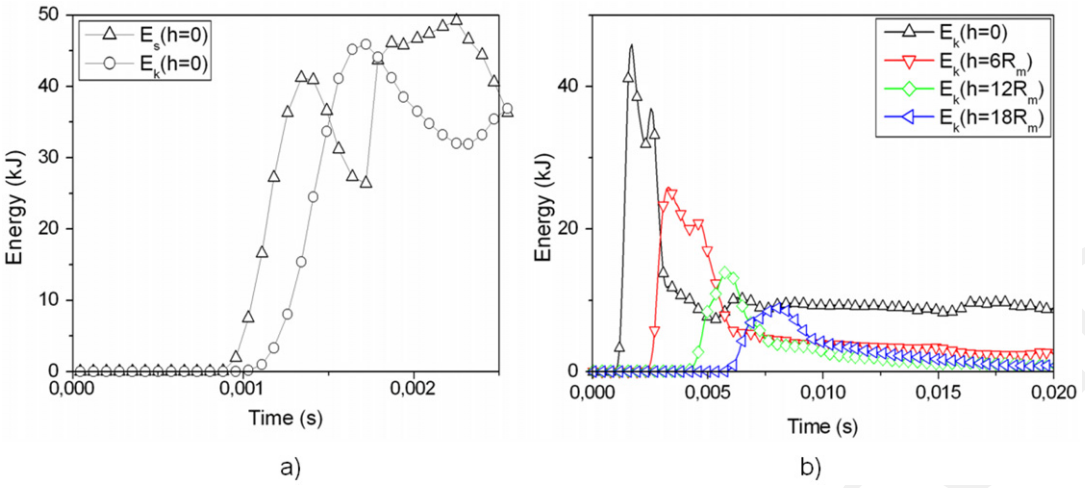

Fig. 2. (a) Time evolution of the strain energy E_s and of the kinetic energy E_k for the central crown ($h = 0$); (b) Energy propagation associated with time delays in the kinetic energy peaks for crowns located for increasing distances h from the impact point.

2.3. Micromechanical properties of the assembly

For local impact loadings, the material is subjected to very local changes. The classical analyses of the microstructure of granular materials based on statistical quantities [18], such as the distribution of the contacts orientation or of the mean contact force depending on the contact directions, are therefore not well adapted.

On the contrary, the time evolution of the coordination number over different domains provides interesting information on the evolution of the micromechanical properties of the material. The analysis of the contact forces based on two networks [19], called strong and weak force networks respectively, corresponding to contacts associated with larger and smaller contact forces than the average contact force is also relevant. The strong force network is responsible for material resistance and the weak force network ensures stability of force chains associated with the strong force network. In this study, the analysis focuses on the relative number of contacts and on the location of the contacts associated with these two networks.

The time evolutions of the kinetic energies of different groups of particles are also studied using a decomposition of the material particles into two groups related with the two contact forces networks. The particles belonging to these two groups are, respectively, the particles whose maximum contact force is larger than the mean contact force, called strongly loaded particles, and the particles whose maximum contact force is smaller than the mean contact force, called weakly loaded particles. This analysis allows studying whether weakly loaded or strongly loaded particles preferentially move which provide information on the evolution of the intensity of particle displacements in relation with the forces applied on the particles.

3. Energy transfers and material properties changes

The time evolution of the energy transfers and of the material micromechanical properties are analyzed for both short and long durations after the first interaction between the projectile and the material.

The impact of the projectile on the surface of the material is marked by an increase in the strain energy of the material near the impact point directly followed by an increase in its kinetic energy (Fig. 2a). This process is due to an energy transfer from the projectile to the material at the impact point. For concentric crowns located farther and farther from the impact point, the kinetic energy increase are time delayed (Fig. 2b) as the propagation of the energy occurs from the impact point to the limit of the sample.

During the initial energy propagation from the impact point to the limit of the sample, the kinetic energy of strongly loaded and weakly loaded particles inside a given concentric crown do not evolve at the same time. The beginning of the propagation of the energy inside a given domain (concentric crown located at $h = 12R_m$ from the impact point for Fig. 3) is associated with the increase in the kinetic energy of strongly loaded particles. This phase is followed by a decreasing phase correlated with the increase in the kinetic energy of strongly loaded particles into the neighboring domain located farther from the impact point (concentric crown located at $h = 18R_m$ from the impact point for Fig. 3). The decrease in the kinetic energy of strongly loaded particles is also correlated with an increase in the kinetic energy of weakly loaded particles (Fig. 3). After the energy propagation to the limit of the material sample, the kinetic energy is significant for any domain considered, and in particular near the impact point ($Ec(h = 0)$ – Fig. 2b). The remaining kinetic energy is mainly associated with weakly loaded particles. Indeed, after energy propagation, the kinetic energy of strongly loaded particles reaches very small values (Fig. 3).

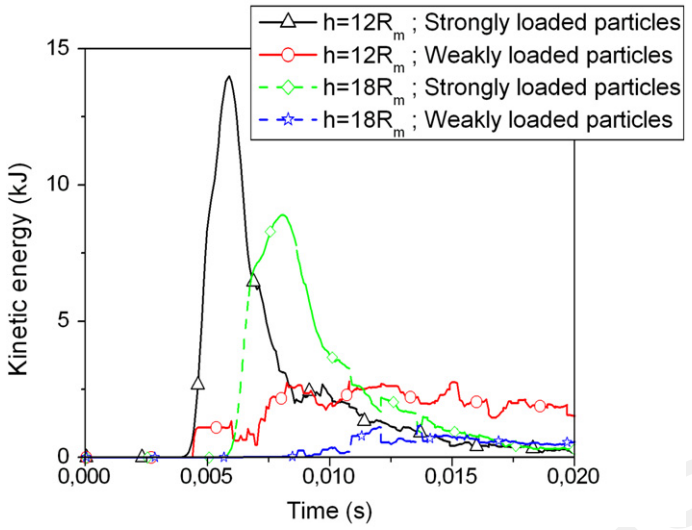

Fig. 3. Time evolution of the kinetic energy associated with strongly loaded and weakly loaded particles for the concentric crowns located at $h = 12R_m$ and at $h = 18R_m$ from the impact point.

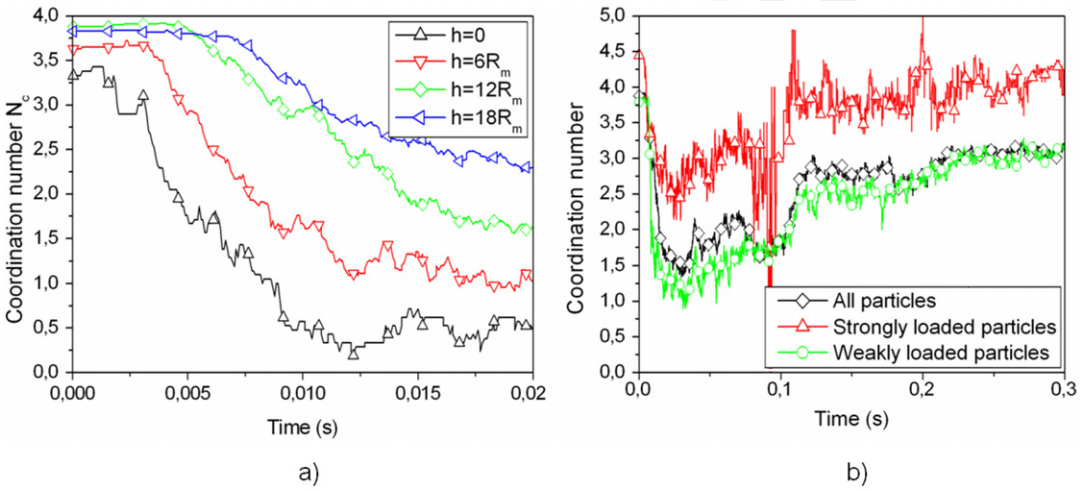

Fig. 4. (a) Time evolution of the coordination number over concentric crowns centered on the impact point; (b) Time evolution of the coordination number of strongly loaded, weakly loaded and all particles for the concentric crown located at $h = 12R_m$ from the impact point.

Complementary with the analysis on the kinetic energy transfers inside the material, a detailed study of the evolution of the micromechanical properties of the material is performed. First, the evolution of the coordination number is studied for all particles and for weakly and strongly loaded particles separately. The simulations show that the energy propagation is associated with a rapid and important decrease in the coordination number (Fig. 4a). The disturbance in the coordination number is less significant for crowns located at increasing distances from the impact point (Fig. 4a). The decrease in the coordination number is followed by an increasing phase which is very long compared to the previous phase (Fig. 4b; Fig. 7a). One can note that the time evolution of the coordination number is similar for both strongly and weakly loaded particles (Fig. 4b).

The evolution of the coordination number is closely related to the evolution of the number of contacts both in the weak and strong force networks, with the number of contact exchanges between the two networks and with the number of contact openings. The following analysis focuses on the evolution of the contact numbers, contact exchanges and contact openings inside a concentric crown located at $h = 12R_m$ from the impact point to facilitate the correlation of the results with the energy propagation phase.

The energy propagation, that is the kinetic energy peak (Fig. 3), is correlated with a decrease in the total number of contacts (Fig. 5a). This decrease is mainly due to the decrease in the number of contact associated with the weak force network (Fig. 5a). On the contrary, the number of contacts associated with the strong force network increases (Fig. 5a) when the kinetic energy of the strongly loaded particles increases (Fig. 3) inside the domain. Following this phase, a decrease in

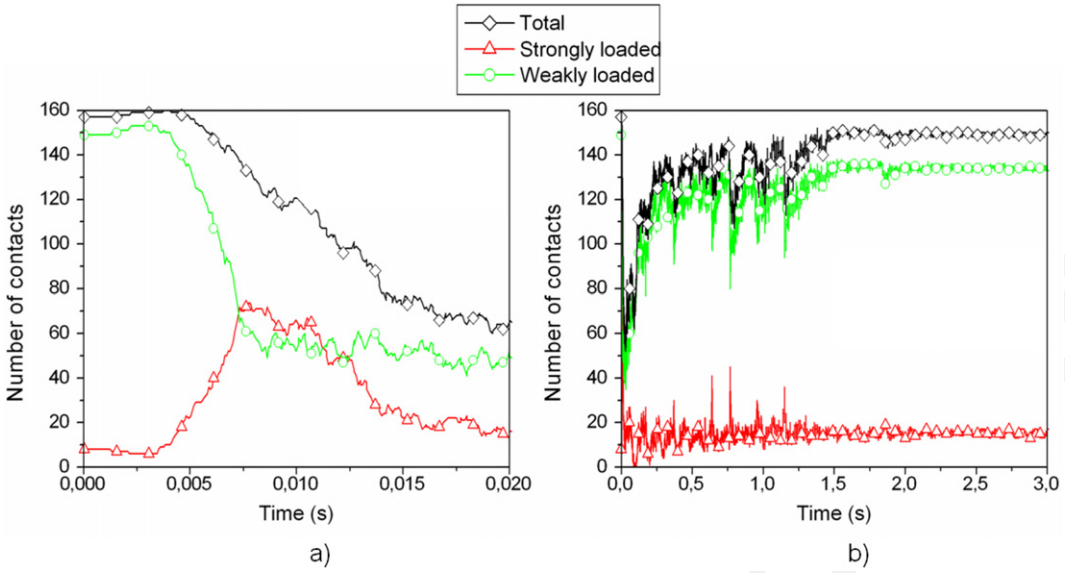

Fig. 5. Time evolution of the total number of contacts and of the number of contacts associated with, respectively, strong and weak force networks for the concentric crown located at $h = 12R_m$ from the impact point and for both short (a) and long (b) durations.

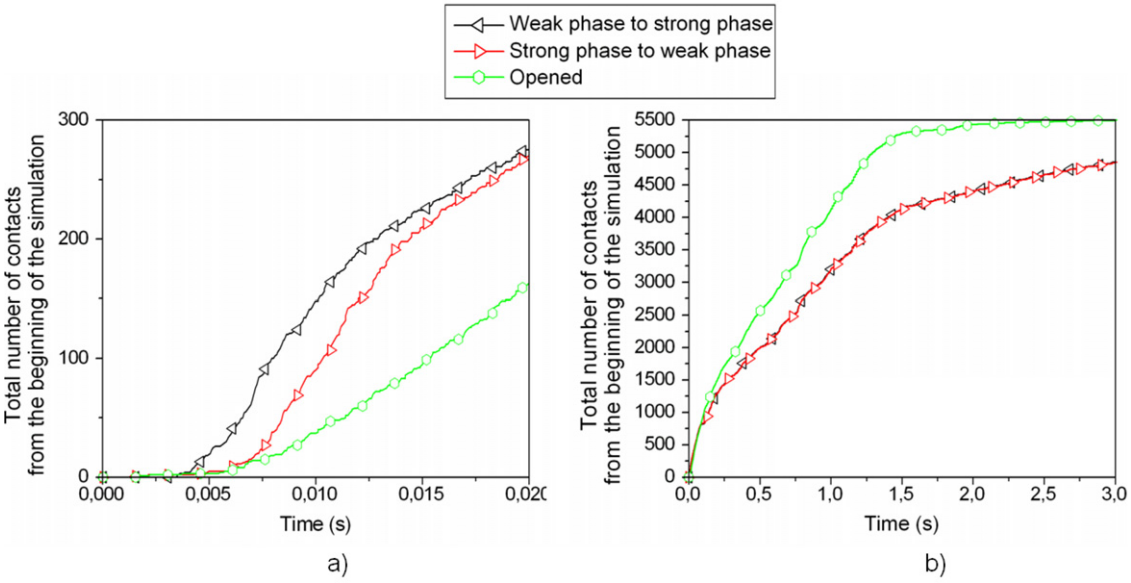

Fig. 6. Concentric crown located at $h = 12R_m$ from the impact point: total number of contact from the beginning of the simulation which were transferred from the strong force network to the weak force network, from the weak force network to the strong force network and which were opened for short (a) and long (b) durations.

the number of strong contacts is observed after energy propagation through the domain (Fig. 5a; Fig. 3). For long durations, one can note that, as for the coordination number (Fig. 4; Fig. 7a), a slow increase in the number of contacts associated with the weak force networks (Fig. 5b) is observed after this fast decreasing phase.

The variations in the number of contacts can be explained by both transfers between the two contact networks and by contact openings (Fig. 6). In the simulations, the number of contact transfers and contact openings between two timesteps is depending on the amplitude of the timestep. To suppress this dependency, the total number of contact transfers and contact openings from the beginning of the simulation are tracked instead of the number of transfers and openings per timestep. The values of the total numbers of transfers and openings are nil at the beginning of the simulation and increase during the simulation. The total number of transfers from the weak phase to the strong phase starts increasing (Fig. 6a) when the kinetic energy starts increasing inside a given domain (Fig. 3). On the contrary, the transfers from the strong phase to the weak phase and contact openings only start increasing (Fig. 6a) after energy propagation through the domain,

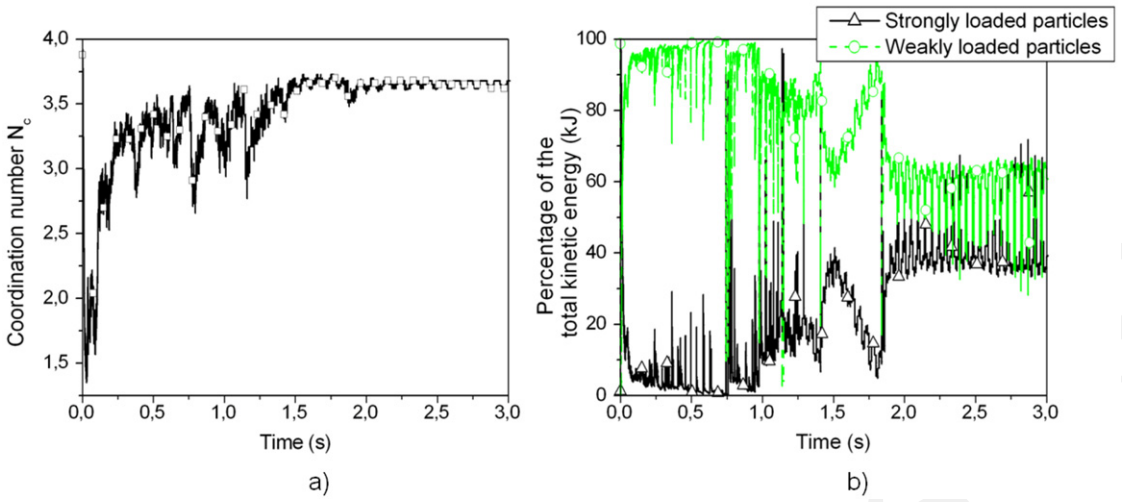

Fig. 7. Time evolution of the coordination number (a) and of the percentage of the total kinetic energy associated with strongly and weakly loaded particles (b) for a concentric crown located at $h = 12R_m$ from the impact point and for long durations.

that is when the energy starts increasing into a neighboring domain located farther from the impact point than the domain considered (Fig. 3). After the time delay between the initial increase in the numbers of contact transfers between the two force networks, the total numbers of contact transfers between the two networks reach the same value and evolve in the same manner (Fig. 6a). For long durations ($t > 2$ s – Fig. 6b), contact transfers between the two networks persist whereas the total number of contact openings reaches a stable value which means that contact openings stop. Finally, one can note that the stopping of contact openings is closely related with a stabilization of the coordination number (Fig. 7a) and with a sudden change in the relative part of the total kinetic energy associated with the strongly and weakly loaded particles (Fig. 7b). For long durations, the relative parts of the kinetic energy associated with the strongly and weakly loaded particles vary in a quasi-periodical way.

4. Successive mechanisms induced by the impact

The time evolution of the kinetic energy inside the material allows differentiating two successive phases. First, the energy introduced during the impact propagates from the impact point to the limit of the sample leading to significant kinetic energy in any domain of the material sample. Second, the kinetic energy is slowly dissipated for any domain considered. This phase corresponds to the balance recovery of the material. The relative durations of these two phases are very different. The initial energy propagation is a short term process compared with the balance recovery phase.

4.1. Short-term energy propagation

The initial energy exchange from the projectile initiates the propagation of the energy inside the material. The energy propagates through the existing contact chains similarly to a wave. The impact of the projectile first entails the formation of disturbing contact forces on the impacted material particles. These disturbing forces F_o are very large compared with the previously existing contact forces F_c (Fig. 8; $F_o \gg F_c$). As demonstrated for a column of bead [20–22] (Fig. 8), the intensity of the disturbing force F_o strongly governs the motion of the loaded particle and on the occurrence of the contact opening. For $F_o \gg F_c$, the high disturbing force induces first the fast motion of the loaded particle and second the opening of the loaded contact. The fast motion of the particle is associated with a fast and important increase in its kinetic energy. On the contrary, for $F_o \sim F_c$, the motion of the loaded particle occurs slowly and no contact opening is observed. The increase in the kinetic energy of the loaded particles is therefore smaller.

At the beginning of the simulation, the high disturbing contact forces due to the impact of the projectile result in significant motions of the loaded particles and in openings of the loaded contacts. These phenomena explain the kinetic energy peak, correlated with a coordination number decrease first observed in the vicinity of the impact point. The high disturbing forces propagate through the existing force chains from the impact point. Fast motions of the loaded particles and contacts openings of the loaded contacts therefore occur with time delay for increasing distances from the impact point which explains the observed time-delayed energy peaks, correlated with significant coordination number decreases. As a consequence, when the disturbing forces reach the limit of the sample, the complete material is associated with significant kinetic energies and small coordination numbers.

One can note that the effects of the high disturbing forces are the less pronounced from domains located the farther from the impact point both in terms of kinetic energy peak intensity and coordination number decrease. This is due to

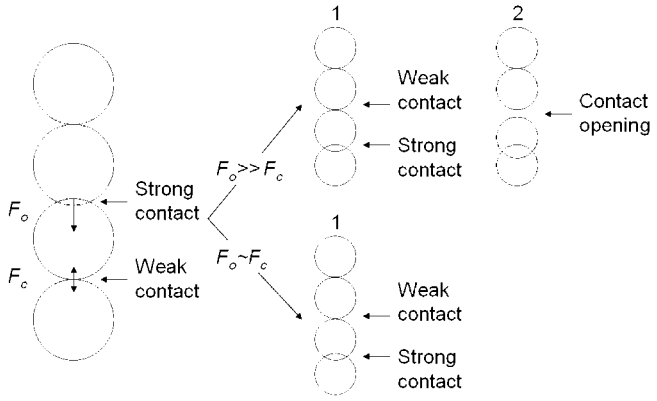

Fig. 8. Transfer between weak and strong contact force network and occurrence of contact openings depending on the relative intensities of the disturbing force applied on the contact F_o and of the existing contact force F_c.

less important intensities of the disturbing forces F_o compared with the mean contact force F_c that can be explained by the following reasons. First, for increasing distances from the impact point, the energy dissipation, which induces lower disturbing forces, is more and more pronounced. Second, for geometrical reasons, the number of loaded contacts gets larger for increasing distances from the impact point which entails a smaller disturbing force per loaded contact. Third, as the material was generated under gravitational processes, the initial mean contact force F_c increases for increasing distances from the material surface, that is from the impact point, which leads to smaller relative importance of the disturbing forces compared with the existing contact forces.

4.2. Long-term balance recovery

The initial propagation of the energy induces the loss of static equilibrium of the material. This propagation phase will therefore be followed by a balance recovery phase.

After the energy propagation through the material, the kinetic energy of the material is significant. Most of the particles of the material are therefore significantly moving. In addition, the coordination numbers of both strongly and weakly loaded particles are small. The balance recovery phase consists in a slow decrease in the kinetic energy of the material correlated with a slow increase in the coordination number.

The balance recovery requires the formation of new stable forces' networks. Just after energy propagation through the material, the important numbers of contact openings and contact transfers between the two force networks show that stable contacts networks do not exist. The disturbing forces are still too important compared with the surrounding forces (Fig. 8). In addition, although the kinetic energy of strongly loaded particles is very reduced, the weakly loaded particles, related with the weak contact force network, are still moving and the weak network cannot fulfill its stabilizing effect [19] on the contact chains. The contact chains can therefore not reach equilibrium.

The creation of permanent force chains is only observed when contact openings stop which is the case for long durations ($t > 2$ s in the case studied). The stopping of contact openings is related with the decrease in the disturbing forces that reach values of the same order as the mean contact force ($F_o \sim F_c$; Fig. 8). The creation of permanent force chains is correlated with the stabilization of the coordination number and with the decrease in the number of contact exchanges between the two contact networks. Although the contact chains are formed, particles belonging to the chains are still moving inducing contact exchanges between the two contact networks without contact openings. The motion of the particles also induces quasi-periodic energy exchanges between strongly and weakly loaded particles. These exchanges may persist while the total amount of the energy transferred from the projectile to the material is not dissipated. For the simulations performed, the dissipation of the complete energy may by a long process. Indeed, in the numerical model, energy dissipation is only possible by frictional processes since no plastic or viscous dissipation processes were modelled.

5. Conclusion

The analysis of the impact of a particle on a granular material using a Discrete Element Method model shows that the impact results in the introduction of energy inside the material. The energy introduced first propagates from the impact point to the limit of the sample through the existing force chains. After energy propagation, the kinetic energy is significant and the contact force chains are broken for any domain of the material. After this phase, the kinetic energy decreases due to frictional dissipation processes. The energy decrease is associated with a long recovery balance phase that results in the creation of new stable contact forces networks. The balance recovery phase can be separated into two successive phases. First, the motion of weakly loaded particles and the numerous contact openings prevent the formation of stable force chains. Second, contact openings stop and stable chains are formed. However, for the duration of the simulations, the

Accepted Manuscript

complete equilibrium of the material sample is not reached because contact exchanges still exist between the two contact networks although contact openings are stopped.

References

[1] W. Goldsmith, Impact: The Theory and Physical Behaviour of Colliding Solids, Edward Arnold (Publishers) Ltd., London, 1960.
[2] M. Frémond, Rigid bodies collisions, Phys. Lett. A 204 (1995) 33–41.
[3] C. Thornton, Z. Ning, A theoretical model for the stick/bounce behaviour of adhesive, elastic–plastic spheres, Powder Technol. 99 (1998) 154–162.
[4] W.J. Stronge, Impacts Mechanics, Cambridge University Press, Cambridge, 2000.
[5] K. Tanaka, M. Nishida, T. Kunimochi, T. Takagi, Discrete element simulation and experiment for dynamic response of two-dimensional granular matter to the impact of a spherical impacting particle, Powder Technol. 124 (2002) 160–173.
[6] M.P. Ciamarra, A.H. Lara, A.T. Lee, D.I. Goldman, I. Vishik, H.L. Swinney, Dynamics of drag and force distributions for projectile impact in a granular medium, Phys. Rev. Lett. 92 (194301) (2004) 1–4.
[7] L. Oger, M. Ammi, A. Valance, D. Beladjine, Discrete element method to study the collision of one rapid sphere on 2D and 3D packings, Eur. Phys. J. E 17 (2005) 467–476.
[8] J. Crassous, D. Beladjine, A. Valance, Impact of a projectile on a granular medium described by a collision model, Phys. Rev. Lett. 99 (24) (2007) 248001.
[9] M. Toiya, J. Hettinga, W. Losert, 3D imaging of particle motion during penetrometer testing. From microscopic tomacroscopic soil mechanics, Granular Matter 9 (2007) 323–329.
[10] S. Deboeuf, P. Gondret, M. Rabaud, Dynamics of grain ejection by sphere impact on a granular bed, Phys. Rev. E 79 (4) (2009) 041306.
[11] F. Bourrier, F. Nicot, F. Darve, Physical processes within a 2D granular layer during an impact, Granular Matter 10 (2008) 415–437.
[12] Itasca, PFC^{2D} – Theory and Background, Itasca, 1999.
[13] P.A. Cundall, O.D.L. Strack, A discrete numerical model for granular assemblies, Geotechnique 29 (1) (1979) 47–65.
[14] P.A. Cundall, Computer simulations of dense spheres assemblies, in: B.V.M. Satake, J.T. Jenkins (Eds.), Micromechanics of Granular Materials, Elsevier Science Publisher, 1988, pp. 113–123.
[15] R.D. Mindlin, H. Deresiewicz, Elastic spheres in contact under varying oblique forces, J. Appl. Mech. 20 (1953) 327–344.
[16] R.E. Goodman, Introduction to Rock Mechanics, PWS Publishing Company, 1980.
[17] L.K.A. Dorren, F. Berger, U.S. Putters, Real-size experiments and 3D simulation of rockfall on forested and non-forested slopes, Nat. Hazards Earth Syst. Sci. 6 (1) (2006) 145–153.
[18] B. Cambou, in: B. Cambou, M. Jean (Eds.), Micromechanics of Granular Materials, Wiley and Sons, 2001.
[19] F. Radjai, D.E. Wolf, M. Jean, J.-J. Moreau, Bimodal character of stress transmission in granular packings, Phys. Rev. Lett. 80 (1998) 61–64.
[20] C. Coste, E. Falcon, S. Fauve, Solitary waves in a chain of beads under Hertz contact, Phys. Rev. E 56 (5) (1997) 6104–6117.
[21] C.S. Campbell, A problem related to the stability of force chains, Granular Matter 5 (2003) 129–134.
[22] S. Job, F. Melo, A. Sokolow, S. Sen, Solitary wave trains in granular chains: experiments, theory and simulations, Granular Matter 10 (2007) 13–20.

Accepted Manuscript